Progress In Electromagnetics Research, PIER 64, 167–189, 2006

WIRE ANTENNA MODEL FOR TRANSIENT ANALYSIS OF SIMPLE GROUNDING SYSTEMS, PART II: THE HORIZONTAL GROUNDING ELECTRODE

D. Poljak and V. Doric

Department of electronics
University of Split
Split, Croatia

Abstract—In the Part I of this work general introduction to the transient impedance assessment of simple grounding systems has been presented. Part I also deals with the analysis of the vertical grounding electrode, while this paper analyses a more demanding case of the horizontal electrode. The mathematical model is based on the thin wire antenna theory featuring the Pocklington integro-differential equation. The Pocklington equation is solved using the Galerkin-Bubnov indirect Boundary Element Method. The details are available in Appendix. The formulation of the problem is posed in the frequency domain, while the corresponding transient response of the grounding system is obtained by means of the inverse Fourier transform. Some illustrative numerical results are shown throughout this work.

1. INTRODUCTION

Transient electromagnetic behaviour of horizontal grounding electrode is of widespread interest in protection of electrical and electronic systems [1–4]. In Part I of this work [5] the transient analysis of vertical grounding electrode has been carried out. The mathematical model presented there employs the thin wire antenna theory, Pocklington integral equation for buried wires with a modified kernel to account for the earth-air interface reflected electromagnetic field, as well as the usual infinite's medium Green function.

This paper deals with the transient impedance calculation of the horizontal grounding electrode, respectively, as a simple grounding systems. In principle, the procedure presented in this paper is quite similar to the one for the vertical electrode though the parts of

formulation regarding the current distribution and input impedance are more demanding in the case of horizontal wire.

This model also poses problem in the frequency domain, and transient analysis of the grounding systems is obtained by applying the inverse Fourier transform, while the linear surge-protection components are modelled in the time domain. In general, it is not easy to collect these models [4].

Recently, a direct time domain analysis of a straight wire antenna embedded in a dielectric half-space has been presented in [6] and can be regarded as an opener to the subject. Further work on the subject will deal with the full time domain model including the ground conductivity.

The method presented in this paper is based on the Pocklington integro-differential equation formulation [1, 6] and related reflection coefficient approximation to account for the presence of a lossy half-space (instead of analytically demanding and numerically time consuming Sommerfeld integral approach [1, 7, 9]).

The current along the horizontal grounding electrode is obtained by solving the corresponding integro-differential equation via the indirect scheme of the Galerkin-Bubnov Boundary Element Method (GB-BEM) [9–11].

The feed point voltage can be obtained by analytically integrating the normal electric field from the electrode surface to infinity.

The input impedance of the horizontal electrode is obtained as a ratio of evaluated voltage and injected current at the feed point.

The frequency response of the electrode is obtained multiplying the input impedance spectrum with Fourier transform of the given lightning current waveform.

Finally, the transient impedance of the horizontal grounding electrode is computed by means of the inverse Fourier transform.

Some illustrative numerical results for the input impedance spectrum and transient impedance are presented in the paper.

2. INTEGRAL EQUATION FOR THE CURRENT ALONG THE HORIZONTAL ELECTRODE

The horizontal grounding electrode is represented by the straight end-fed wire of length L and radius a, buried in a lossy medium at depth d as shown in Fig. 1. The electrode is assumed to be perfectly conducting and its dimensions satisfy the well known thin wire approximation [1, 7, 9–11].

The Pocklington integro-differential equation for the horizontal electrode can be derived by expressing the electric field in terms of

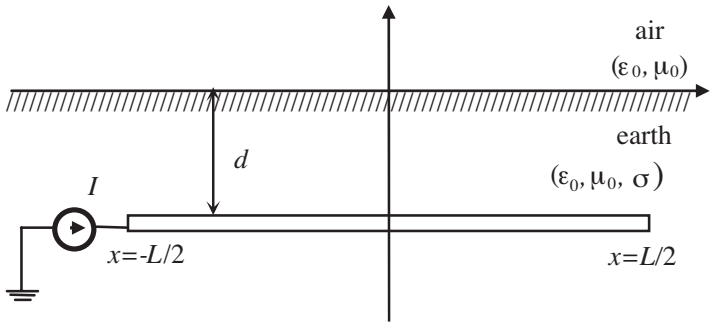

Figure 1. Horizontal grounding wire energized by a current source I_g.

the Hertz vector potential and by satisfying the appropriate boundary conditions for the tangential field components at the electrode surface, in the same manner as it was done for vertical electrode.

The complete electric field induced in the vicinity of the straight thin wire of finite length buried in an imperfectly conducting half-space can be expressed in terms of Hertz vector potential Π [8]:

$$\vec{E} = \nabla\left(\nabla\vec{\Pi}\right) + k_1^2\vec{\Pi} \tag{1}$$

where k_1 is the phase constant of a lossy ground:

$$k_1^2 = -\omega^2\mu\varepsilon_{eff} \tag{2}$$

and ε_{eff} denotes the complex permittivity of the lossy ground:

$$\varepsilon_{eff} = \varepsilon_r\varepsilon_0 - j\frac{\sigma}{\omega} \tag{3}$$

where and ε_r and σ are relative permittivity and conductivity of the ground respectively, and ω denotes the operating frequency.

A corresponding integral equation formulation for the horizontal grounding electrode using Sommerfeld and RC approach is presented in Subsections 2.1 and 2.2, respectively.

2.1. Sommerfeld Integral Approach

The scattered tangential electric field in the vicinity of the straight horizontal thin wire buried at depth d in the earth expressed by vector Equation (1), can be written in terms of the Hertz vector potential components Π_x and Π_z [6]:

$$E_x^H(x,z) = \left[\frac{\partial^2}{\partial x^2} + k_1^2\right]\Pi_x^H + \frac{\partial^2\Pi_z^H}{\partial x\partial z} \tag{4}$$

$$E_z^H(x,z) = \frac{\partial^2 \Pi_z^H}{\partial x \partial z} + \left[\frac{\partial^2}{\partial z^2} + k_1^2\right] \Pi_z^H \tag{5}$$

where superscript H emphasize the horizontal grounding electrode electrode.

The vector potential components for the straight horizontal buried wire are given by [7]:

$$\Pi_x^H = \frac{1}{j4\pi\omega\mu\varepsilon_{eff}} \int_{-L/2}^{L/2} \left[g_0^H(x,x',z) - g_i^H(x,x',z) + U_{11}\right] I(x')dx' \tag{6}$$

$$\Pi_z^H = \frac{1}{j4\pi\omega\varepsilon_{eff}} \int_{-L/2}^{L/2} \frac{\partial W_{11}}{\partial x} I(x')dx' \tag{7}$$

where $I(x')$ is current distribution along the wire, $g_0^H(x,x',z)$ denotes the free space Green function of the form:

$$g_0^H(x,x',z) = \frac{e^{-jk_1 R_{1h}}}{R_{1h}} \tag{8}$$

while $g_i^H(x,x',z)$ arises from the image theory and is given by:

$$g_i^H(x,x',z) = \frac{e^{-k_2 R_{2h}}}{R_{2h}} \tag{9}$$

where R_{1h} and R_{2h} are the distances from the horizontal wire in the lossy ground and from its image in the air to the observation point in the lower medium, respectively.

The influence of the imperfectly conducting ground is taken into account by the attenuation terms in the form of Sommerfeld integrals U_{11} and W_{11}, defined as follows [1]:

$$U_{11} = 2\int_0^\infty \frac{e^{-\mu_1(d-z)}}{\mu_1+\mu_2} J_0(\lambda\rho)\lambda d\lambda \tag{10}$$

$$W_{11} = 2\int_0^\infty \frac{(\mu_1-\mu_2)e^{-\mu_1(d-z)}}{k_2^2\mu_1 + k_1^2\mu_2} J_0(\lambda\rho)\lambda d\lambda \tag{11}$$

where $J_0(\lambda\rho)$ is zero order Bessel function of the first kind, while μ_1, μ_2 and ρ are given by:

$$\mu_1 = \left(\lambda^2 - k_1^2\right)^{1/2}, \qquad \mu_2 = \left(\lambda^2 - k_1^2\right)^{1/2} \qquad \rho = |x - x'| \tag{12}$$

Assuming the perfectly conducting wire [1, 7], the total tangential electric field, vanishes along the perfectly conducting electrode surface, i.e.,

$$E_x^{exc,H}(x,a) + E_x^{sct,H}(x,a) = 0 \tag{13}$$

where $E_z^{exc,H}$ is the excitation function and $E_z^{sct,H}$ is the corresponding scattered field along the electrode surface.

Taking into account the Sommerfeld integrals property:

$$\frac{\partial W_{11}}{\partial z} = k_1^2 V_{11} - U_{11} \tag{14}$$

Combining the relations (4) to (14) yields:

$$E_x^{exc,H} = -\frac{1}{j4\pi\omega\varepsilon_{eff}} \left\{ \int_{-L/2}^{L/2} \frac{\partial^2}{\partial x^2} \left[g_0^H(x,x') - g_i^H(x,x') + k_1^2 V_{11} \right] I(x')dx' + k_1^2 \int_{-L/2}^{L/2} \left[g_0^H(x,x') - g_i^H(x,x') + U_{11} \right] I(x')dx' \right\} \tag{15}$$

Solving the integral Equation (15) the current distribution along the horizontal electrode is obtained.

2.2. Simplified Reflection Coefficient Approach

The evaluation of the Sommerfeld integrals (10), (11) is rather difficult task [1, 7, 9]. Namely, this approach requires repeated evaluation of Sommerfeld integrals and matrix inversion on several frequencies, for spectrum calculation purposes which is rather time consuming.

A simplified approach based on the modified image theory was proposed in [2] for handling the grounding systems and in [12] for the treatment of the plane wave coupling to horizontal buried cables. However, the modified image theory is based on a quasi-static approximation of the phenomena and takes into account only the electrical properties of the soil but not the burial depth as a parameter.

This work deals with a reflection coefficient (RC) approach by which the angle of electric field reflection from the earth-air interface and the burial depth of the grounding electrode are both taken into account. The principal advantage of the RC approach versus rigorous Sommerfeld integral approach is a simplicity of the formulation and significantly less computational cost.

For convenience, the integro-differential Equation (15) can be written in the form:

$$E_x^{exc} = -\frac{1}{j4\pi\omega\varepsilon_{eff}} \int_{-L/2}^{L/2} G^H(x,x')I(x')dx' \tag{16}$$

where $G(x,x')$ is the total Green function given by:

$$\begin{aligned} G^H(x,x') &= \frac{\partial^2}{\partial x^2}\left[g_0^H(x,x') - g_i^H(x,x') + k_1^2 V_{11}\right] \\ &\quad + k_1^2\left[g_0^H(x,x') - g_i^H(x,x') + U_{11}\right] \end{aligned} \tag{17}$$

According to the RC approximation the simplified Green function for the horizontal grounding electrode is given by:

$$\begin{aligned} G^H(x,x') &= \left[\frac{\partial^2}{\partial x^2} + k_1^2\right]\left[g_0^H(x,x') - g_i^H\Gamma(x,x')\right] \\ &= \left[\frac{\partial^2}{\partial x^2} + k_1^2\right] g^H(x,x') \end{aligned} \tag{18}$$

while Γ is the corresponding reflection coefficient for the TM polarization [11]:

$$\Gamma = \frac{\frac{1}{\underline{n}}\cos\theta - \sqrt{\frac{1}{\underline{n}} - \sin^2\theta}}{\frac{1}{\underline{n}}\cos\theta + \sqrt{\frac{1}{\underline{n}} - \sin^2\theta}} \tag{19}$$

where θ and $\underline{n}$ are given by:

$$\theta = \operatorname{arctg}\frac{|x-x'|}{2d}; \qquad \underline{n} = \frac{\varepsilon_{eff}}{\varepsilon_0} \tag{20}$$

Also, the Pocklington integro-differential equation for the straight horizontal wire buried in the lossy ground is:

$$E_x^{exc,H} = -\frac{1}{j4\pi\omega\varepsilon_{eff}} \int_{-L/2}^{L/2} \left[\frac{\partial^2}{\partial x^2} + k_1^2\right]\left[g_0^H(x,x') - \Gamma g_i^H(x,x')\right] I(x')dx' \tag{21}$$

Solving the integral Equation (21) via Galerkin-Bubnov indirect Boundary Element Method the equivalent current distribution along

the horizontal electrode is obtained. The mathematical details are available in Appendix.

Though the RC approximation is found to be an asymptotically correct form of the Sommerfeld integrals in the far-field region the relationship between the rigorous and approximate field expressions is not in general so simple [8].

On the other hand the RC approach provides a more efficient algorithm compared to the rigorous method. One possible way of doing a trade off between the approximate and rigorous approach could be the comparison of numerical results, rather than analytical considerations [5, 8].

2.3. Imposed Boundary Conditions

In the analysis of the grounding electrodes, the excitation function cannot be defined in the form of an incident electric field, as this field vanishes along the perfectly conducting (PEC) wire surface, i.e.,

$$E_x^{exc} = 0 \tag{22}$$

so the integral Equation (15) and (21) have become homogeneous [1, 7].

The horizontal grounding electrode is energized by the injection of a current pulse of an arbitrary waveform produced by an ideal current source with one terminal connected to the grounding electrode with the other one grounded at infinity.

The excitation can be defined by the current flowing into the wire. This current source is incorporated into the integral equation scheme through the boundary condition:

$$I(-L/2) = I_g \tag{23}$$

where I_g denotes the current generator.

This unit current source is often used in the frequency domain calculations as it is the counterpart of the time domain current pulse.

3. THE EVALUATION OF THE INPUT IMPEDANCE SPECTRUM

As the horizontal grounding electrode is represented by the wire antenna model the calculation of antenna input impedance against the grounding system input impedance presented in this work should be discussed and a corresponding trade off should be made.

The calculation of the wire antenna input impedance is relatively a simple task, because the terminal points of the voltage generator are

very close, i.e., one deals with the so-called delta-function generator [1, 7].

The calculation of grounding system input impedance is more demanding than in the antenna case, primarily because the input terminals are placed between ground electrode point and remote soil, and the integration on the infinite integral cannot be avoided.

The input impedance is given by the ratio:

$$Z_{in} = \frac{V_g}{I_g} \tag{24}$$

where V_g and I_g are the values of the voltage and the current at the driving point.

The feed-point voltage can be calculated by integrating the normal electric field component from the electrode surface to infinity, i.e.:

$$V_g = -\int_{\infty}^{a} \vec{E} d\vec{s} \tag{25}$$

Hence, as in the case of vertical electrode the problem of obtaining the input impedance is referred to the calculation of feed-point voltage. The input impedance spectrum is obtained by repeating this this procedure in the wide frequency band.

For the case of horizontal grounding electrode the integral (25) becomes:

$$V_g = -\int_{\infty}^{a} E_z^H(x,z) dz \tag{26}$$

The radial electric field component, normal to the electrode, is now given by:

$$E_z^H(x,z) = \frac{\partial^2 \Pi_x^H}{\partial x \partial z} = \frac{1}{j4\pi\omega\varepsilon_{eff}} \int_{-L/2}^{L/2} I(x') \frac{\partial^2 g^H(x,x',z)}{\partial x \partial z} dx' \tag{27}$$

The kernel G^H has the following symmetry property:

$$\frac{\partial g^H(x,x',z')}{\partial x} = -\frac{\partial g^H(x,x',z)}{\partial x'} \tag{28}$$

and performing the integration by parts expression (28) becomes:

$$E_z(x,z) = -\frac{1}{j4\pi\omega\varepsilon_{eff}} \frac{d}{dz} \left[I(x') g^H(x,x',z) \Big|_{x'=-L/2}^{x'=L/2} \right.$$

$$- \int_{-L/2}^{L/2} \frac{\partial I(x')}{\partial x'} g^H(x, x', z) dx' \Bigg] \tag{29}$$

It can be observed that the differentiation over x variable is avoided while a differentiation over z variable, is replaced outside the integral sign.

Substituting the Equation (29) into (26) it follows:

$$\begin{aligned} V_g &= -\frac{1}{j4\pi\omega\varepsilon_{eff}} \int_a^{\infty} \frac{d}{dz} \Bigg[I(x') g^H(x, x', z) \Big|_{z'=-L/2}^{z'=L/2} \\ &\quad - \int_{-L/2}^{L/2} \frac{\partial I(x')}{\partial x'} g^H(x, x', z) dx' \Bigg] dz \end{aligned} \tag{30}$$

simply leading to:

$$\begin{aligned} V_g &= \frac{1}{j4\pi\omega\varepsilon_{eff}} \Bigg[I(-L/2) g^H(x, -L/2, z) \\ &\quad - \int_{-L/2}^{L/2} \frac{\partial I(x')}{\partial x'} g^H(x, x', z) dx' \Bigg] \Bigg|_{z=a}^{z=\infty} \end{aligned} \tag{31}$$

The tedious numerical integration over infinite domain in (31) is avoided and the desired input impedance of the buried wire is determined by the relation:

$$\begin{aligned} Z_{in} &= \frac{1}{j4\pi\omega\varepsilon_{eff} I_g} \Bigg[I(-L/2) g^H(x, -L/2, z) \\ &\quad - \int_{-L/2}^{L/2} \frac{\partial I(x')}{\partial x'} g^H(x, x', z) dx' \Bigg] \Bigg|_{z=a}^{z=\infty} \end{aligned} \tag{32}$$

However, the approximation of Sommerfeld integrals with Fresnel reflection coefficient (RC) should be performed very carefully, and validity limits of this approach should be clarified, as well.

The Sommerfeld integral approach has found to be numerically stable for buried horizontal wire brought to within 10^{-6} wavelengths of the interface [6–8]. In addition, the RC approach produces results roughly within 10% of these obtained via rigorous Sommerfeld integral approach.

3.1. The Transient Impedance Calculation

The transient impedance of the horizontal grounding electrode is defined as a ratio of time varying voltage and current at the input terminals [1]:

$$z(t) = \frac{v(t)}{i(t)} \tag{33}$$

where $i(t)$ is the current injected at an end of the horizontal electrode, Fig. 1.

This injected current is related to the lightning channel current given by:

$$i(t) = I_0 \cdot \left(e^{-\alpha t} - e^{-\beta t}\right), \qquad t \geq 0 \tag{34}$$

where pulse rise time is determined by constants α and β, while I_0 denotes the amplitude of the current waveform.

The calculation procedure for $v(t)$ is the same as in the case of the vertical electrode and the details are available in Part I of this work [5].

4. NUMERICAL RESULTS

Figures 2 and 3 show the frequency spectrum of the input impedance for the grounding electrode of length $L = 1\,\mathrm{m}$, and radius $a = 5\,\mathrm{mm}$, buried at depth $d = 1\,\mathrm{m}$ in the ground with $\varepsilon_r = 10$. Ground conductivity is $\sigma = 0.001\,\mathrm{S/m}$ (dry sand, gravel) and $\sigma = 0.01\,\mathrm{S/m}$ (loam, clay), respectively. The obtained results are compared with results available from [13]. The agreement between results calculated via different approaches is found to be satisfactorily.

Fig. 4 shows the transient impedance for the grounding electrode of same dimensions buried at depth $d = 1\,\mathrm{m}$ compared to the results from [13].

Grounding electrode is excited by the double exponential current pulse with parameters $I_0 = 1.1043\,\mathrm{A}$, $\alpha = 0.07924 \cdot 10^6\,\mathrm{s}^{-1}$, $\beta = 4.0011 \cdot 10^6\,\mathrm{s}^{-1}$. The agreement is judged to be satisfactorily again.

At this point, the choice of the parameters α and β are determined by rise time (time-to-maximum value of the current waveform) and duration time (time-to-half maximum). Thus, values $\alpha = 0.07924 \cdot 10^6 s^{-1}$, $\beta = 4.0011 \cdot 10^6 s^{-1}$ correspond to time-to-maximum $1\,\mu\mathrm{s}$ and time-to-half maximum $10\,\mu\mathrm{s}$ [13, 14].

This excitation current pulse is chosen in a way to be as close as possible to the realistic lightning pulse. In realistic scenarios the rise time of the current pulse varies from $0.1\,\mu\mathrm{s}$ to a few $\mu\mathrm{s}$, while the

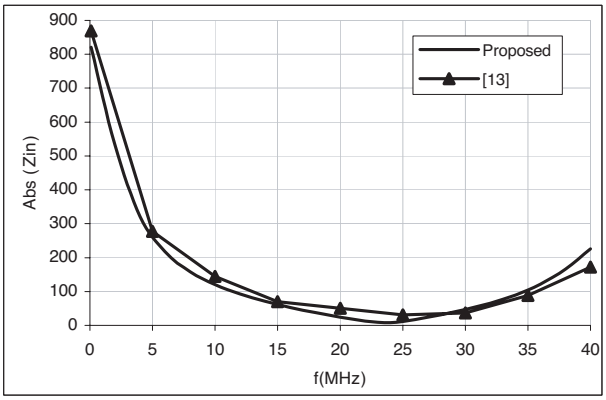

Figure 2. Input impedance spectrum of the grounding electrode: $L = 1\,\mathrm{m}$, $a = 5\,\mathrm{mm}$, $d = 1\,\mathrm{m}$, $\varepsilon_r = 10$, $\sigma = 0.001\,\mathrm{S/m}$.

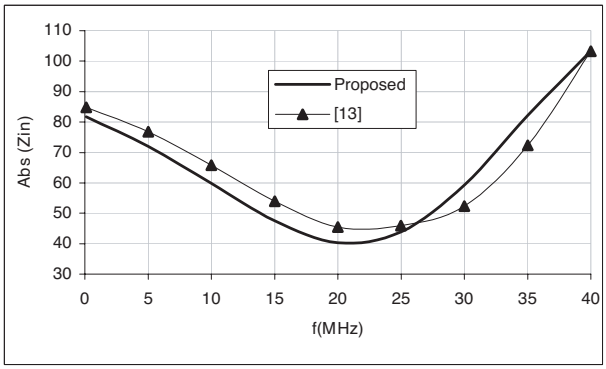

Figure 3. Input impedance spectrum of the grounding electrode: $L = 1\,\mathrm{m}$, $a = 5\,\mathrm{mm}$, $d = 1\,\mathrm{m}$, $\varepsilon_r = 10$, $\sigma = 0.01\,\mathrm{S/m}$.

duration time, defined as a time required for the current magnitude decrease to the 50% of maximal value ranges from $5\,\mu$s to $2000\,\mu$s.

The computational details regarding the use of inverse Fourier Transform have already discussed in Part I of this work [5].

Fig. 5 and 6 show the input impedance spectra for horizontal grounding electrode of length $L = 1\,\mathrm{m}$ and $L = 10\,\mathrm{m}$, respectively buried at depth $d = 0.5\,\mathrm{m}$ in the lossy ground with $\varepsilon_r = 10$ and conductivity $\sigma = 0.00185\,\mathrm{S/m}$ (specific resistivity $\rho = 5400\,\Omega\mathrm{m}$).

Fig. 7 shows the frequency spectrum of the lightning strike current

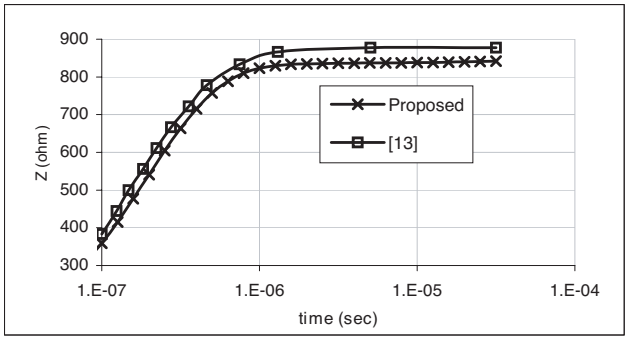

Figure 4. Transient impedance of the grounding electrode buried in the lossy ground: $L = 1\,\mathrm{m}$, $a = 5\,\mathrm{mm}$, $d = 1\,\mathrm{m}$, $\varepsilon_r = 10$, $\sigma = 0.001\,\mathrm{S/m}$.

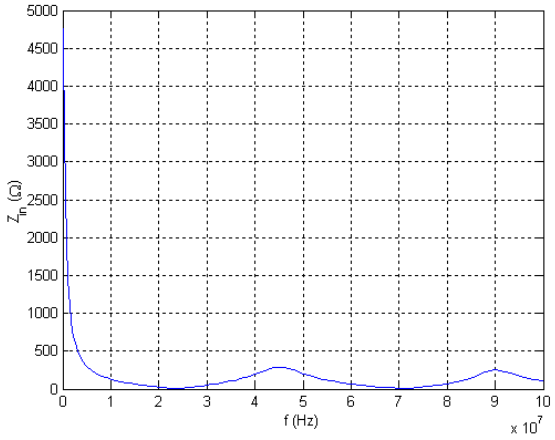

Figure 5. Input impedance spectrum ($L = 1\,\mathrm{m}$, $d = 0.5\,\mathrm{m}$, $\rho = 5400\,\Omega\mathrm{m}$).

pulse. It is visible that this pulse practically vanishes for frequencies higher than 2 MHz. However, to obtain the proper information about the early time behaviour of the transient response higher harmonics need to be taken into account. As the Inverse Fast Fourier Transform (IFFT) requires $\Delta t = 1/2f_{\max}$ it follows for $f_{\max} = 100\,\mathrm{MHz}$, $\Delta t = 5\,\mathrm{ns}$.

The frequency spectrum of the voltage induced at the grounding electrode input is obtained by multiplying the input impedance

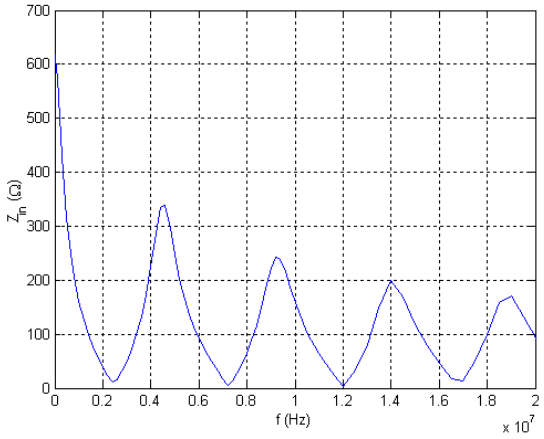

Figure 6. Input impedance spectrum ($L = 10\,\mathrm{m}$, $d = 0.5\,\mathrm{m}$, $\rho = 5400\,\Omega\mathrm{m}$).

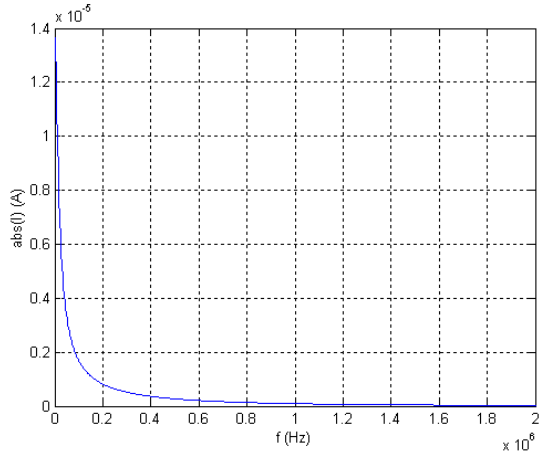

Figure 7. Frequency spectrum of the current pulse.

spectrum and the spectrum of the current pulse. Applying the IFFT the transient voltage at the input of the grounding electrode is obtained. Fig. 8 shows the normalized injected current and induced voltage waveform for the horizontal grounding electrode of length $L = 1\,\mathrm{m}$. A shift between the current excitation function and induced voltage clearly demonstrates the reactive character of the grounding impedance, contrary to the widely adopted assumption of the resistive

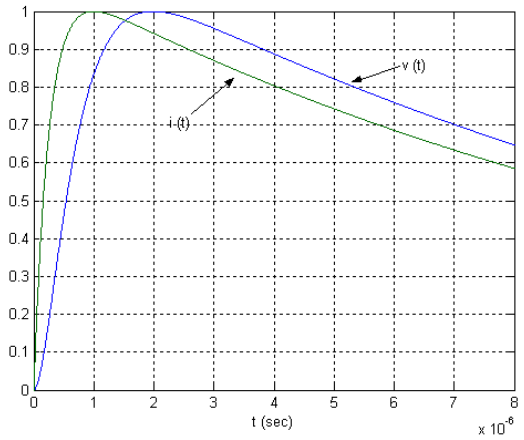

Figure 8. Normalized values of the current pulse and induced voltage.

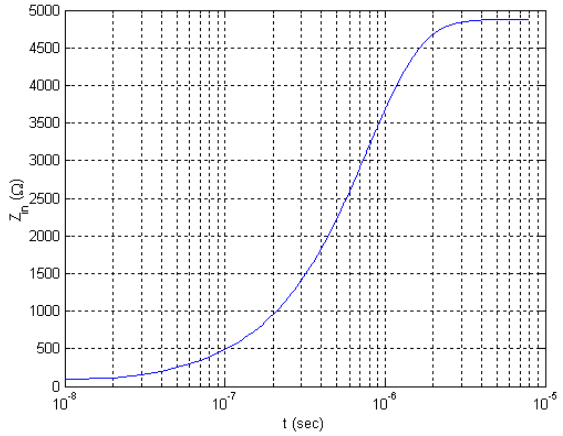

Figure 9. Transient impedance of the horizontal grounding electrode: $L = 1\,\mathrm{m}$, $d = 0.5\,\mathrm{m}$, $\rho = 5400\,\Omega\mathrm{m}$.

grounding electrode behavior.

The ratio of time dependent voltage and current gives the transient impedance of the grounding electrode. Figures 9 to 11 show the transient impedance waveform for various electrode lengths. It is obvious that greater is the conductor length the lower is the value of the transient impedance. Generally, the transient impedance at instant $t = 0$ has the zero value and reaches the stationary value after some time. The waveform presented in Fig. 11 is due to the signal reflection

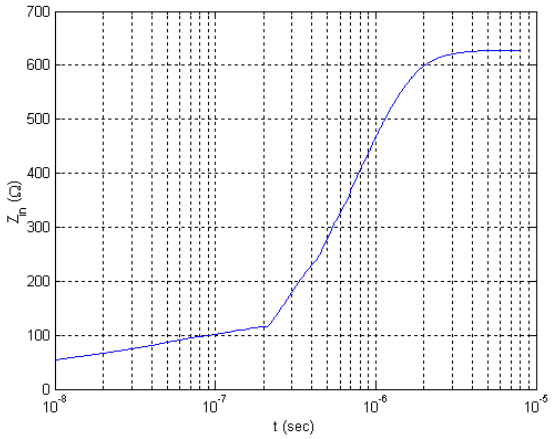

Figure 10. Transient impedance of the horizontal grounding electrode: $L = 10\,\mathrm{m}$, $d = 0.5\,\mathrm{m}$, $\rho = 5400\,\Omega\mathrm{m}$.

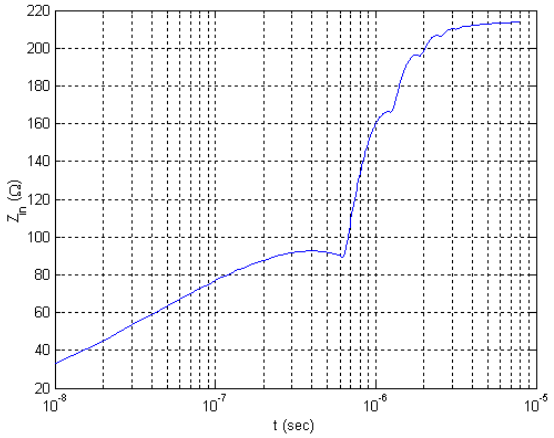

Figure 11. Transient impedance of the horizontal grounding electrode: $L = 30\,\mathrm{m}$, $d = 0.5\,\mathrm{m}$, $\rho = 5400\,\Omega\mathrm{m}$.

from the wire ends. The physical explanation to the differences in the values of the transient impedance visible in Fig. 9 to 11 is related to the energy loss of the grounding electrode due to the radiation mechanism. Namely, in accordance to the implemented model arising from the thin wire antenna theory the horizontal grounding electrode behaves as the end-driven antenna immersed in a lossy medium.

Figure 12 shows the results for the various burial depths. It is

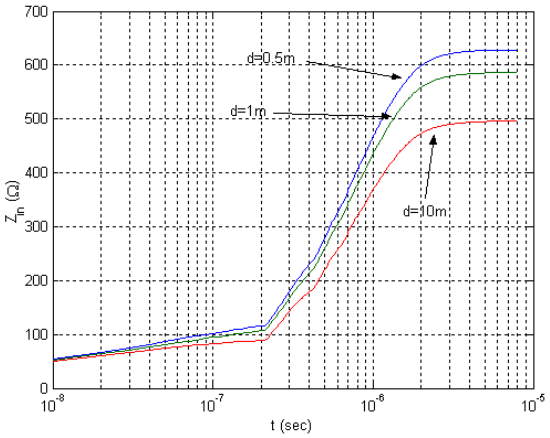

Figure 12. Transient impedance of the horizontal grounding electrode: $L = 10\,\mathrm{m}$, $\rho = 5400\,\Omega\mathrm{m}$.

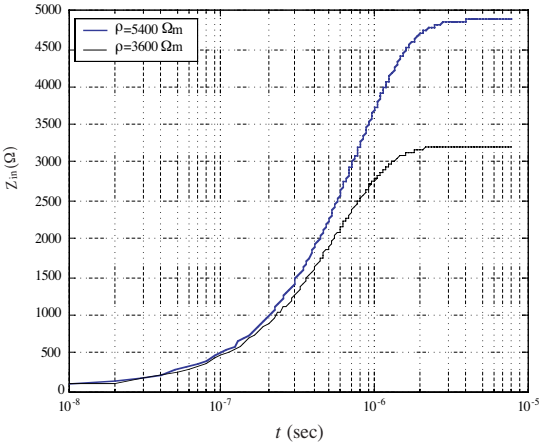

Figure 13. Transient impedance of the horizontal grounding electrode: $L = 1\,\mathrm{m}$, $d = 0.5\,\mathrm{m}$.

visible that the impedance decreases as the burial depth increases. In particular, the impedance reaches the lowest value at $d = 10\,\mathrm{m}$ where the influence of the earth-air interface is negligible. In realistic case the soil at greater burial depth may have a higher humidity which would additionally decrease of the input impedance.

In Fig. 13 results for two different values of soil resistivity are compared. As expected, a lower value of a soil resistivity implies the

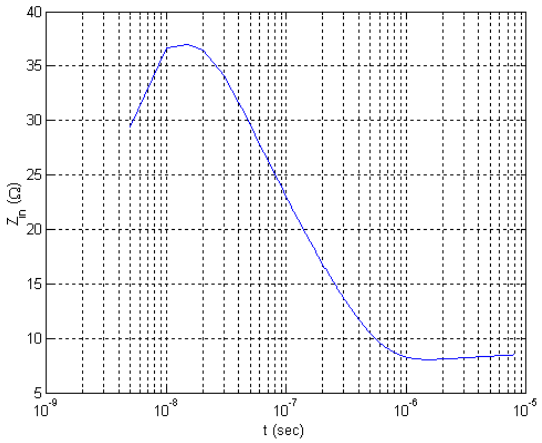

Figure 14. Transient impedance of the horizontal grounding electrode: $L = 10\,\mathrm{m}$, $d = 10\,\mathrm{m}$, $\rho = 100\,\Omega\mathrm{m}$.

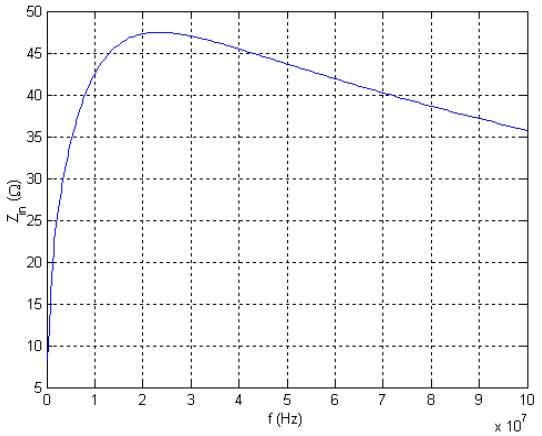

Figure 15. Input impedance spectrum ($L = 10\,\mathrm{m}$, $d = 10\,\mathrm{m}$, $\rho = 100\,\Omega\mathrm{m}$).

lower value of the transient impedance.

In all examples presented so far, the transient impedance continuously grows from zero value to the stationary value (maximum value). Fig. 14 shows a transient impedance wave-form for the case of low soil resistivity. Reached grounding resistance equals $9\,\Omega$. However observing the transient impedance it is obvious that the maximal value of the transient impedance is around $37\,\Omega$, i.e., four times higher. From

this example it is visible that transient impedance calculation is very important especially the early time transient response. The low value of the grounding resistance does not ensure the lightning protection in the case of lightning strike.

Fig. 15 shows the freq. spectrum of the input impedance. Comparing to spectrum shown in Figs. 1 and 2 it is visible that this spectrum is not monotonically decreasing.

5. CONCLUSION

The transient impedance calculation of the horizontal grounding electrode based on the antenna theory approach is presented in this paper. The problem is formulated in the frequency domain while the time domain results are computed by using the inverse Fourier transform.

The horizontal grounding electrode is represented by the straight end-fed wire antenna, buried in a lossy ground.

The equivalent current distribution along the electrode is obtained by solving the corresponding Pocklington integro-differential equation via the indirect Galerkin-Bubnov variant of the boundary element method (GB-BEM).

The influence of the nearby earth-air interface is taken into account by the reflection coefficient appearing within the integro-differential equation kernel.

Electric field in the surrounding soil is determined from the previously calculated current distribution. Input impedance is obtained by analytically integrating the radial electrical field from the remote soil to the electrode surface.

The frequency response of the horizontal electrode is obtained by multiplying the Fourier transform of the current pulse with the input impedance spectrum.

The transient impedance of the electrode is computed using the Inverse Fast Fourier Transform (IFFT). Obtained numerical results show that the transient impedance of the horizontal grounding electrode is strongly dependent on the variation of electrode length, its burial depth and the specific resistance of the ground.

The advantage of the proposed RC approach over rigorous approaches based on Sommerfeld integrals is primarily simplicity and computational efficiency. Further extension of this method to the treatment of complex grounding systems consisting of interconnected conductors will be reported subsequently. This analysis is anticipated as Part III of this work.

APPENDIX A. BOUNDARY ELEMENT SOLUTION OF POCKLINGTON INTEGRO-DIFFERENTIAL EQUATION

The Pocklington integro-differential equation types, such as Equation (21), are usually handled by the point matching technique [1, 15] which principal feature is simplicity. However, the point-matching approach suffers from relatively poor convergence rate and the kernel quasisingularity problem also arises [11].

To overcome these disadvantages an indirect Galerkin-Bubnov scheme of the Boundary Element Method is used in this paper. This numerical approach has been promoted in [9], where the method was applied to the problem of dipole antenna radiating over lossy half space.

For the sake of completeness, the numerical method is outlined below.

It is convenient to start this procedure with an operator form of (21) which can be symbolically written as:

$$KI = Y \tag{A1}$$

where K is a linear operator, I is the unknown function to be found for a given excitation Y.

The unknown current is then expanded into a finite sum of n linearly independent basis functions f_i with unknown complex coefficients I_i:

$$I \cong I_n = \sum_{i=1}^{n} I_i f_i \tag{A2}$$

Substituting (A2) into (A1) yields:

$$KI \cong KI_n = \sum_{i=1}^{n} \alpha_i K f_i = Y_n = P_n(Y), \tag{A3}$$

where $P_n(Y)$ is called a projection operator [10]. Now the residual R_n is formed:

$$R_n = KI_n - Y = P_n(Y) - Y. \tag{A4}$$

According to the definition of the scalar product of functions in Hilbert function space the error R_n is weighted to zero with respect to certain weighting functions $\{W_j\}$, i.e.,

$$\langle R_n, W_j \rangle = 0; \qquad j = 1, 2, \ldots, n, \tag{A5}$$

where the expression in brackets denotes:

$$\langle R_n, W_j \rangle = \int_{\Omega} R_n W_j^* d\Omega, \tag{A6}$$

where Ω is the domain of interest.

Since the operator K is linear, one obtains a system of algebraic equations and by choosing $W_j = f_j$ for the case of the Galerkin-Bubnov procedure, yields:

$$\sum_{i=1}^{n} \alpha_i \langle K\ f_i, f_j \rangle = \langle Y, f_j \rangle\ j = 1, 2, \ldots, n. \tag{A7}$$

Equation (A7) is the strong Galerkin-Bubnov formulation of the Pocklington integral Equation of (A1) [9–11]. Utilizing the integral equation kernel symmetry and taking into account the boundary conditions for current at the free ends of the wire, after integration by parts it follows:

$$\begin{aligned} \sum_{i=1}^{n} I_i \frac{1}{j4\pi\omega\varepsilon_{eff}} & \left\{ \begin{array}{l} -\int\limits_{-L/2}^{L/2} \dfrac{df_i(x)}{dx} \int\limits_{-L/2}^{L/2} \dfrac{df_i(x')}{dx'} g^H(x,x')dx'dx \\ -k^2 \int\limits_{-L/2}^{L/2} f_j(x) \int\limits_{-L/2}^{L/2} f_i(x') g^H(x,x')dx'dx \end{array} \right\} \\ = \quad & -\int_{-L/2}^{L/2} E_x^{exc} f_j(x)dx, \quad j = 1, 2, \ldots, n \end{aligned} \tag{A8}$$

Equation (A8) represents the weak Galerkin-Bubnov formulation of the integral equation of (A1).

This approach provides some definite advantages over the commonly used point-matching techniques:

- The second-order differential operator is replaced by trivial derivatives over basis and test (weight) functions thus avoiding the problem of quasi-singularity [9–11].
- The basis and test functions can be chosen arbitrarily. The only requirement to be satisfied by bases and weights is that they must be chosen from the class of order-one differentiable functions.
- The conditions at the wire ends are subsequently incorporated into the global matrix of the linear equation system.

Performing the boundary element discretization the solution for the unknown current $I^e(x)$ along the boundary element can then be written as:

$$I^e(x') = \{f\}^T \{I\} \tag{A9}$$

Assembling the contributions from each element the resulting system of equations is given by:

$$\sum_{i=1}^{M}[Z]_{ji}\{I\}_i = \{V\}_j, \qquad \text{and} \qquad j = 1, 2, \ldots, M \tag{A10}$$

where M is the total number of wire segments and $[Z]_{ji}$ is the mutual impedance matrix representing the interaction of the i-th source boundary element with the j-th observation boundary element:

$$[Z]_{ji} = -\frac{1}{j4\pi\omega\varepsilon_{eff}} \left\{ \begin{array}{l} \int\limits_{\Delta l_j}\int\limits_{\Delta l_i} \{D\}_j\{D'\}_i^T g^H(x,x')dx'dx \\ +k^2 \int\limits_{\Delta l_j}\int\limits_{\Delta l_i} \{f\}_j\{f\}_i^T g^H(x,x')dx'dx \end{array} \right\}. \tag{A11}$$

Matrices $\{f\}$ and $\{f'\}$ contain the shape functions while $\{D\}$ and $\{D'\}$ contain their derivatives, M is the total number of finite elements, and Δl_i, Δl_j are the widths of i-th and j-th boundary elements.

$\{V\}_j$ is the voltage vector for the j-th observation boundary element given by:

$$\{V\}_j = \int\limits_{\Delta l_j} E_x^{exc}\{f\}_j dx, \tag{A12}$$

Throughout this work the linear approximation over a boundary element is used as it has been shown that this choice provides accurate and stable results for various wire configurations [9–11]. Since the functions $f(x)$ are required to be of class C^1 (once differentiable), a convenient choice for the shape functions over the finite elements is the family of Lagrange's polynomials given by:

$$L_i(x) = \prod_{j=1}^{m} \frac{x - x_j}{x_i - x_j}, \qquad j \neq i. \tag{A13}$$

However, the ground wire, represented by the end-fed monopole antenna, considered in this paper is neither excited by voltage generator nor illuminated by plane wave. It is driven at its end by the equivalent current generator, so the right-side vector is equal to zero resulting in the homogeneous linear equation system, , i.e.,

$$\sum_{i=1}^{M}[Z]_{ji}\{I\}_i = 0, \qquad \text{and} \qquad j = 1, 2, \ldots, M \tag{A14}$$

The excitation function in the form of the current generator I_g is taken into account as a forced condition in the first node of the solution vector:

$$I_1 = I_g \tag{A15}$$

and the linear equation system can be properly solved.

REFERENCES

1. Grcev, L. and F. Dawalibi, "An electromagnetic model for transients in grounding systems," *IEEE Trans. Power Delivery,* Vol. 5, No. 4., 1773–1781, Oct. 1990.
2. Grcev, L. D. and F. E. Menter, "Transient electromagnetic fields near large earthing systems," *IEEE Trans. Magnetics,* Vol. 32, 1525–1528, May 1996.
3. Liu, Y., M. Zitnik, and R. Thottappillil, "An improved transmission line model of grounding system," *IEEE Trans. EMC,* Vol. 43, No. 3, 348–355, 2001.
4. Ala, G. and M. L. Di Silvestre, "A simulation model for electromagnetic transients in lightning protection systems," *IEEE Trans. EMC,* Vol. 44, No. 4, 539–534, 2003.
5. Poljak, D. and V. Doric, "An efficient wire antenna model for transient analysis of simple grounding systems, Part I: The vertical grounding electrode," submitted to *IEEE Trans. on PWD.*
6. Poljak, D. and V. Doric, "Time domain modeling of electromagnetic field coupling to finite length wires embedded in a dielectric half-space," *IEEE Trans. EMC,* Vol. 47, No. 3, 247–253, 2005.
7. Poljak, D. and V. Roje, "The integral equation method for ground wire impedance," *Integral Methods in Science And Engineering,* C. Constanda, J. Saranen, S. Seikkala (eds.), Vol. 1, 139–143, Longman, UK, 1997.
8. Burke, G. J. and E. K. Miller, "Modeling antennas near to and penetrating a lossy interface," *IEEE Trans. AP,* Vol. 32, 1040–1049, 1984.
9. Poljak, D., "New numerical approach in the analysis of a thin wire radiating over a lossy half-space," *Int. Journ. Num. Meth. in Engineering,* Vol. 38, No. 22, 3803–3816, Nov. 1995.
10. Poljak, D. and V. Roje, "Boundary element approach to calculation of wire antenna parameters in the presence of dissipative half-space," *IEE Proc. Microw. Antennas Propag.,* Vol. 142, No. 6, 435–440, Dec. 1995.

11. Poljak, D., *Electromagnetic Modelling of Wire Antenna Structures,* WIT Press, Southampton, Boston, 2001.
12. Poljak, D., I. Gizdic, and V. Roje, "Plane wave coupling to finite length cables buried in a lossy ground," *BEM 23*, 185–193, Lemnos Island, Greece, May 7–9, 2001.
13. Grcev, L., "Calculation of the transient impedance of grounding systems," Ph.D. Thesis, University of Zagreb, 1986 (in Croatian).
14. Grcev, L., "Computer analysis of transient voltages in large grounding systems," *IEEE Trans. Power Delivery,* Vol. 11, No. 2, 815–1781, April 1996.
15. Barrera-Figueroa, V., J. Sosa-Pedroza, and J. López-Bonilla, "Simplification of Pocklington's integral equation for arbitrary bent thin wires," *Boundary Elements XXVII (Electrical Engineering and Electromagnetics)*, A. Kassab, C. A. Brebbia, E. Divo, and D. Poljak (eds.), Vol. 39, 563–574, Wessex Institute of Technology Trans. on Modelling and Simulation, WIT Press, UK, 2005.